On MIMO SATCOM Capacity Analysis: Utilising Polarization and Spatial Multiplexing

Balachander Ramamurthy*†, William G. Cowley†, Linda M. Davis† and Gerald Bolding*
*Defence Science and Technology Organisation
Edinburgh, South Australia.
†Institute for Telecommunications Research,
University of South Australia.
Email: Balachander.Ramamurthy@dsto.defence.gov.au

***Abstract*—In this paper we present a MIMO model for a line-of-sight (LOS) satellite communication (SATCOM) channel, utilising orthogonal circular polarizations and spatial diversity from multiple satellites in geostationary orbit. To achieve spatial orthogonality in a LOS SATCOM channel, antenna separation of the order of hundreds of kilometres is required, either on the ground or in space. In this paper we consider small spacing between the ground terminals, and thus large separation between antennas in space by means of multiple satellites. Orbital slots for multiple satellites within two degrees are generally not viable due to adjacent satellite interference (ASI) issues from disadvantaged small user terminals. In this work we show how to benefit with MIMO spatial multiplexing and multiple satellites with closer orbital spaces. In addition to spatial multiplexing, orthogonal polarizations can double the overall bandwidth. In a SISO context, depolarization and cross talk between orthogonal polarizations are often expressed in terms of cross-polar discrimination (XPD) and cross-polar isolation (XPI) respectively. In a MIMO context, we show that polarization orthogonality is of more significance than antenna XPD or XPI. The capacity results show that significant improvement can be achieved with multiple satellites and polarization MIMO compared to conventional SISO SATCOM.**

I. Introduction

The demand for higher satellite communication (SATCOM) data rates from both civilian and military users continues to grow. Since bandwidth is a finite resource, there is a need for higher spectral efficiency per Hertz. The multiple antenna technique popularly known as MIMO (Multiple Inputs and Multiple Outputs) has been very successful in terrestrial wireless. The gains realised from the application of MIMO techniques have generated enough interest to investigate MIMO in satellite communications (SATCOM) [1]. However, a satellite channel is unlike the terrestrial channel in that it usually doesn't exhibit a rich scattering environment. The SATCOM channel especially at X-band[1] frequencies and above is principally dominated by the line of sight (LOS) path.

The absence of scatterers in the SATCOM propagation path may lead to rank deficiency in the spatial MIMO channel matrix. Hence, at first glance it appears that MIMO cannot provide multiplexing gains for LOS SATCOM. However, large geographical antenna separation either at the transmitter or at the receiver has been shown to offer the extra degrees of freedom for spatial multiplexing in LOS channels [2]. In LOS SATCOM, MIMO spatial multiplexing techniques are analysed in [3], [4] and [5]. The authors in these papers utilize special antenna spacing arrangement to obtain a distinct phase relation within the channel matrix.

In addition, by utilizing orthogonal polarizations, the available spatial multiplexing gain can be doubled. Most commonly, right hand circular polarization (RHCP) and left hand circular polarization (LHCP) are the two orthogonal polarizations used in MILSATCOM. The two polarizations are often used simultaneously as two separate SISO systems. Poor cross polar isolation (XPI), largely due to antenna polarization mismatch, can cause severe degradation in communications performance [6]. However, MIMO techniques can be useful to counter XPI degradation [7].

This paper is organised as follows. In section-II a 2×2 polarization model is derived for dual-polarized (DP) antennas. In section-III a system model is presented for uplink MIMO with spatially separated DP antennas and non-regenerative satellites with conventional SISO downlinks. In section-IV capacity analysis results are presented and the conclusion is given in section-V.

II. Antenna Polarization

Most communications antennas radiate linear polarization, except for a few such as the helical antennas with inherent circular polarization. To generate circular polarization using linear excitation methods, two radiating elements placed perpendicular to each other in the horizontal h and vertical v axes are used, with a quarter wavelength excitation delay between them [8]. To generate LHCP, the signal to the v antenna port is delayed by $\frac{\pi}{2}$ or a quarter wavelength relative to the h antenna port. Similarly, to generate RHCP the signal to the h antenna port is delayed by $\frac{\pi}{2}$ or a quarter wavelength relative to the v antenna port [9].

Thus for circular DP antennas, the antenna polarization matrix P is represented by two unit norm polarization column vectors $\mathbf{p}_1$ and $\mathbf{p}_2$ representing LHCP and RHCP respectively.

$$P_{ideal} = [\mathbf{p}_{1,ideal}\ \mathbf{p}_{2,ideal}] = \frac{1}{\sqrt{2}}\begin{bmatrix} 1 & e^{-j\frac{\pi}{2}} \\ e^{-j\frac{\pi}{2}} & 1 \end{bmatrix}. \quad (1)$$

[1]The United States, Australia and other countries use X-band (7.9-8.4 GHz uplink / 7.25-7.75 GHZ downlink) for military purposes.

978-1-5090-0073-9/15/$31.00 ©2015 IEEE

Authorized licensed use limited to: Georgia Institute of Technology. Downloaded on January 12,2023 at 21:22:05 UTC from IEEE Xplore. Restrictions apply.

The electric fields in the horizontal (E_h) and vertical (E_v) axes can be expressed as:

$$\begin{bmatrix} E_h \\ E_v \end{bmatrix} = P \begin{bmatrix} x_1 \\ x_2 \end{bmatrix}, \tag{2}$$

where x_1 and x_2 are the signals at the input ports of the antenna. However, in practice the generated polarization will be elliptical due to antenna excitation errors in amplitude and phase. In addition, the actual antenna orientation with respect to horizontal and vertical axes is as shown in Figure 1 (dashed lines show the antenna elements). The displacement angles θ_1 and θ_2 are measured with respect to the horizontal and vertical axes respectively. The antenna polarization model with all mismatch factors is then:

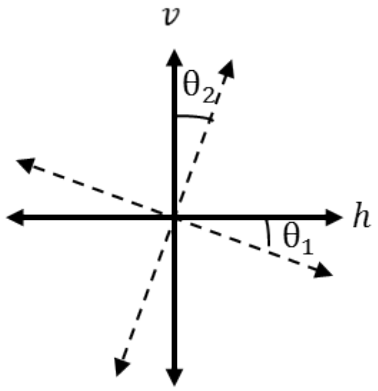

Fig. 1. Antenna orientation with respect to the h and v axes

$$P = [\mathbf{p}_1\ \mathbf{p}_2] = \begin{bmatrix} \cos\theta_1 & \sin\theta_2 \\ -\sin\theta_1 & \cos\theta_2 \end{bmatrix} \begin{bmatrix} A_1 & e^{-j(\frac{\pi}{2}+\psi_2)} \\ e^{-j(\frac{\pi}{2}+\psi_1)} & A_2 \end{bmatrix} \begin{bmatrix} \frac{1}{\sqrt{1+A_1^2}} & 0 \\ 0 & \frac{1}{\sqrt{1+A_2^2}} \end{bmatrix}. \tag{3}$$

The first 2×2 matrix models the antenna orientation. In an ideal case θ_1 will be equal to θ_2. However, for $\theta_1 \neq \theta_2$ the two polarizations are no longer orthogonal. The second 2×2 matrix denotes circular polarization excitation errors in phase (ψ_1 and ψ_2) and amplitude (A_1 and A_2). For an ideal case we have $\psi_1 = \psi_2 = 0$ and $A_1 = A_2 = 1$. The last 2×2 scaling matrix ensures that the two polarization column vectors $\mathbf{p}_1$ and $\mathbf{p}_2$ are unit norm.

The two polarizations are orthogonal if their inner product is zero, i.e., $\mathbf{p}_1$ is orthogonal to $\mathbf{p}_2$ iff $\mathbf{p}_1^\dagger \mathbf{p}_2 = 0$. For DP antennas, the measure of polarization orthogonality p is a vital parameter also referred as polarization paralleity in [10].

$$p = \frac{|\mathbf{p}_1^\dagger \mathbf{p}_2|}{\|\mathbf{p}_1\|\|\mathbf{p}_2\|} \qquad (0 \leq p \leq 1). \tag{4}$$

The polarization orthogonality can be expressed in-terms of polarization excitation errors as:

$$p = \frac{|\sin(\theta_2-\theta_1)(A_1A_2 + e^{j(\psi_1-\psi_2)}) - j(A_1e^{-j\psi_2} - A_2e^{j\psi_1})|}{\sqrt{(1+A_1^2)(1+A_2^2)}}. \tag{5}$$

Irrespective of errors in circular excitation and antenna orientation, the polarization orthogonality p of a DP antenna can be fully orthogonal ($p = 0$) iff $\theta_1 = \theta_2$ and $A_1e^{-j\psi_2} = A_2e^{j\psi_1}$.

A DP antenna with non-zero orthogonality will experience power loss due to mutual coupling between the polarizations. This power loss is analogous to the mutual coupling effect from close inter-element spacing in antenna arrays [11]. Due to a common phase centre between the two polarizations, a DP antenna cannot offer array gain and the polarization matrix has to be scaled in the following way [10]. This is equivalent to scaling the polarization matrix by its maximum eigenvalue.

$$\hat{P} = \frac{P}{\sqrt{1+p}}. \tag{6}$$

The overall polarization matrix denoted by Σ, that includes the transmit antenna, polarization coupling in the channel and the receive antenna is:

$$\Sigma = \hat{P}_r \begin{bmatrix} \sqrt{1-\alpha} & \sqrt{\alpha} \\ \sqrt{\alpha} & \sqrt{1-\alpha} \end{bmatrix} \hat{P}_t, \tag{7}$$

where α is related to channel depolarization effects and the subscripts t and r denote transmit and receive antennas respectively. In a clear sky LOS SATCOM, we assume negligible depolarization in the channel, and α is approximately zero. Hence the polarization state of the overall link is mostly dominated by the antennas.

Often in SISO systems, the cross polar isolation (XPI) is widely used when signals are transmitted simultaneously in opposite polarization. XPI is a measure of how much energy from the opposite polarization (cross-polar) interferes the co-polar signal. In SISO systems, poor XPI often results from polarization misorientation between the antennas [6]. However in a MIMO context, for non-ideal circularly polarized antennas, performance is insensitive to polarization misorientation between the antennas, as long as $\theta_2 = \theta_1$ for each antenna.

III. System Model

Consider an uplink MIMO channel and SISO downlink from each satellite to its respective anchor station. In the uplink, N transmit DP antennas are arranged in an uniform linear array (ULA) separated by distance d_T. In this model $M = 2$ satellites are used, each with a DP antenna on the uplink and a DP antenna on the downlink. Similarly $M = 2$ DP anchor stations are used. Typical orbital spacing between the satellites is in the range $0.5^o \leq d_S \leq 2^o$. An example of the model is shown in Figure 2 with $N = M = 2$.

The overall channel matrix includes the uplink $H_u \in \mathcal{C}^{2M\times 2N}$, the satellite $H_s \in \mathcal{C}^{2M\times 2M}$ and the downlink

Authorized licensed use limited to: Georgia Institute of Technology. Downloaded on January 12,2023 at 21:22:05 UTC from IEEE Xplore. Restrictions apply.

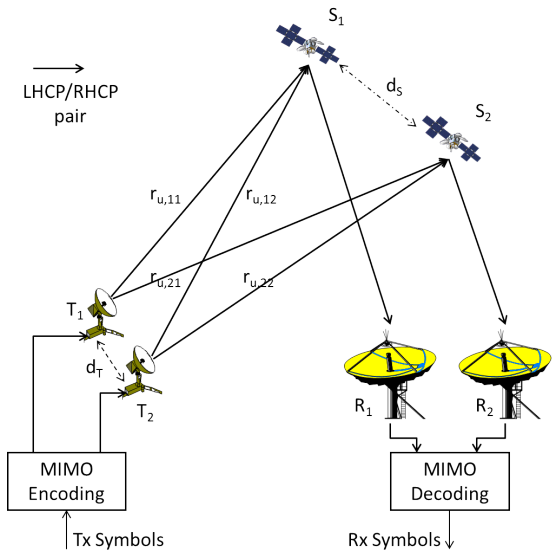

Fig. 2. System model for 4×4 uplink MIMO channel

$H_d \in \mathcal{C}^{2M\times 2M}$ channel components. The uplink MIMO channel in matrix form for $N = M = 2$ is:

$$H_u = \begin{bmatrix} H_{u,11} & H_{u,12} \\ H_{u,21} & H_{u,22} \end{bmatrix}, \tag{8}$$

where,

$$H_{u,mn} = a_{u,mn}\; g_{u,mn}\; \Sigma_{u,mn} e^{-j\phi_{u,mn}} \quad \{m,n = 1,2\}, \tag{9}$$

$$\phi_{u,mn} = 2\pi \frac{f_u}{c} r_{u,mn}, \tag{10}$$

$$g_{u,mn} = g^{pa}_{u,n}\; g^{\text{tx,ant}}_{u,n}\; g^{\text{rx,ant}}_{u,m}. \tag{11}$$

The subscript u denotes the uplink, a denotes the free space path attenuation, g denotes the combined tx/rx antenna gains, r denotes the range in metres, ϕ is the phase offset in the channel, f is the carrier frequency, c denotes speed of light and Σ denotes the 2×2 polarization component from (7). Similarly the downlink channel matrix is given by:

$$H_d = \begin{bmatrix} H_{d,11} & 0_{2\times 2} \\ 0_{2\times 2} & H_{d,22} \end{bmatrix}, \tag{12}$$

where,

$$H_{d,mm} = a_{d,mm}\; g_{d,mm}\; \Sigma_{d,mm} e^{-j\phi_{d,mm}} \quad m = 1,2, \tag{13}$$

$$g_{d,mm} = g^{\text{tx,ant}}_{d,m}\; g^{\text{rx,ant}}_{d,m}, \tag{14}$$

where the subscript d denotes the downlink. The non-regenerative satellite is assumed ideal with an orthogonal matrix:

$$H_s = g^{\text{sr}}_s I_{2M}, \tag{15}$$

$$g^{\text{sr}}_s = g^{\text{rx,lnb}}_s\; g^{\text{tx,pa}}_s, \tag{16}$$

where, g^{sr}_s denotes the satellite repeater gain and we assume equal gain through all satellite channel paths. The overall transfer function of the system is:

$$Y = H_d H_s H_u X + H_d H_s W_u + W_d \tag{17}$$

where, $H_t = H_d H_s H_u$ denotes the overall channel matrix. $X \in \mathcal{C}^{2N\times 1}$ and $Y \in \mathcal{C}^{2M\times 1}$ are the transmit and receive signals respectively. The noise on the uplink from the satellite receive antennas and the noise on the downlink from the anchor receive antennas are white Gaussian noise denoted by $W_u \sim \mathcal{CN}(0, \sigma_u^2 I_{2M})$ and $W_d \sim \mathcal{CN}(0, \sigma_d^2 I_{2M})$ respectively.

A. SVD processing

The singular value decomposition (SVD) technique is a tool widely used in MIMO theory to understand the rank or the degree of freedom of the channel. The SVD technique assumes the overall channel matrix (H_t) is known both at the transmitter and receiver [2]. Using SVD the channel matrix can be decomposed as follows:

$$H_t = U \Lambda V^{\dagger}, \tag{18}$$

where $U \in \mathcal{C}^{2M\times 2M}$, $V \in \mathcal{C}^{2N\times 2N}$ are unitary matrices, and $\Lambda \in \Re^{2M\times 2N}$ is a singular value matrix. The diagonal elements of Λ are non-negative real valued eigenvalues ($\lambda_1 \geq \lambda_2 ... \geq \lambda_k$) and the off diagonal elements are zeros, where k signifies the number of non-zero eigenvalues or the channel rank.

The SVD system model is shown in Figure 3. By substituting (18), $X = V\tilde{X}$ and $\tilde{Y} = U^{\dagger}Y$ in (17) we obtain:

$$\tilde{Y} = U^{\dagger}U\Lambda V^{\dagger}V\tilde{X} + U^{\dagger}H_d H_s W_u + U^{\dagger}W_d, \tag{19}$$

$$= \Lambda\tilde{X} + \tilde{W}_u + \tilde{W}_d. \tag{20}$$

Since U is an unitary matrix, the distribution of $\tilde{W}_d$ will be same as W_d. The distribution of $\tilde{W}_u$ is dependent on the orthogonality of $H_d H_s$ matrix. In this work since we assume an ideal satellite and downlink channel such that $H_d H_s = I_{2M}$, the distribution of $\tilde{W}_u$ will be same as W_u. A non-orthogonal downlink channel effects the $\tilde{W}_u$ distribution. This is outside the scope of this paper, but will be analysed in our future work.

B. Capacity analysis

The capacity of the channel is given by [2]:

$$C = \sum_{i=1}^{k} \log_2\left(1 + \frac{\tilde{S}_i}{\sigma_u^2 + \sigma_d^2}\lambda_i^2\right) \quad \text{bits/s/Hz.} \tag{21}$$

Let $\tilde{S}$ denote total transmit signal power before the V matrix and S denote power after the V matrix. Since V is unitary, $\tilde{S} = S$ so we can write:

$$\tilde{S} = \sum_{i=1}^{k} \tilde{S}_i = \sum_{n=1}^{N} S_n = S. \tag{22}$$

The total transmit signal power is constant irrespective of total number of transmit antennas (N), and allocated with

Authorized licensed use limited to: Georgia Institute of Technology. Downloaded on January 12,2023 at 21:22:05 UTC from IEEE Xplore. Restrictions apply.

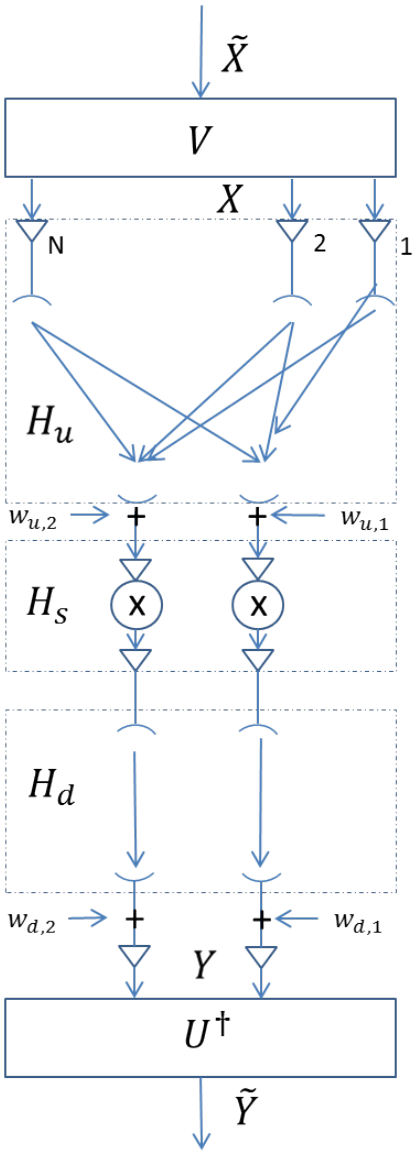

Fig. 3. SVD system model

respect to the rank k of the channel. Power allocation using the water-filling method is an optimum strategy to maximize capacity [2].

$$\tilde{S}_i = \left(\mu - \frac{\sigma_u^2 + \sigma_d^2}{\lambda_i^2}\right)^+, \tag{23}$$

where μ is a parameter to satisfy the total power constraint in (22) and $(x)^+$ denotes $\max\{0, x\}$.

C. Spatial diversity

From [3], [5], to achieve spatial orthogonality in LOS SATCOM channel, antenna separation of the order of hundreds of kilometres is required, either on the ground or in space. In this paper we consider small spacings d_T between the ground terminals, and thus large separations between the antennas in space by using multiple satellites. Optimization for channel orthogonality leads to satisfying the following criteria in channel path lengths [3].

$$(r_{u,1i} - r_{u,1l}) + (r_{u,2l} - r_{u,2i}) = (l-i)\frac{\nu}{N}\frac{c}{f_u} \qquad \nu \nmid N, \tag{24}$$
$$i, l = 1..N,$$

where $\nu \nmid N$ denotes that ν is an integer indivisible by N. The optimal location contour for $N = 2$ is shown in Figure 4. This satisfies equation (24) and places the second terminal (T2) at either of the sides from T1 for $\nu = 1, 3$. The calculations assume two satellites at 156°E and 157°E respectively, uplink in X-band at 8.15 GHz, and a ground transmitting location at 35°S latitude and 138°E longitude. The contour lines and the optimum d_T changes with respect to the geographical location of the transmitters and the satellite orbital locations.

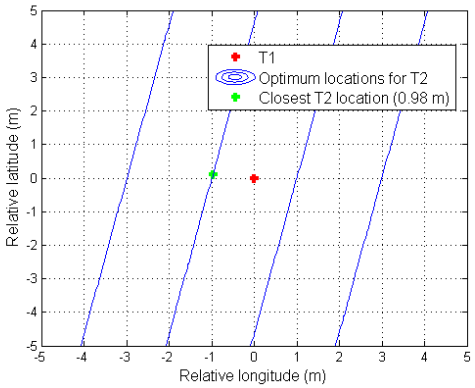

Fig. 4. Optimal location contour for T2 with respect to T1

IV. Results

The rank of the the overall channel matrix for orthogonal polarizations and two satellites cannot be greater than four. In our analysis the antennas are arranged in an uniform linear array (ULA) along the longitudinal axis with d_T spacing between the antennas. The achievable capacity using the SVD technique and the water-filling power allocation method is shown in Figure 5 with respect to d_T and N. To simplify the analysis, the gain and the free-space attenuation factors in the overall channel matrix are unit normalized. The total signal-to-noise ratio is given by SNR $= \frac{\tilde{P}}{\sigma_u^2 + \sigma_d^2}$. The larger N, less the capacity results are prone to antenna miss-positioning error in d_T. This result agrees with analysis presented in [3]. At non-optimum d_T values, for example at 2m and 4m separations, the water-filling power allocation algorithm (23) ceases allocating power to low eigenvalue channel streams. The incremental capacity obtained with more transmit antennas N is an additional benefit of the power gain. The incremental capacity gain is due to the channel state information available at the transmitter (CSIT) and for high SNRs it can be calculated as in [12], with the multiplicative factor 2 from the two polarizations.

$$\Delta C = \max\left(2M \log_2\left(\frac{N}{M}\right), 0\right). \tag{25}$$

Authorized licensed use limited to: Georgia Institute of Technology. Downloaded on January 12,2023 at 21:22:05 UTC from IEEE Xplore. Restrictions apply.

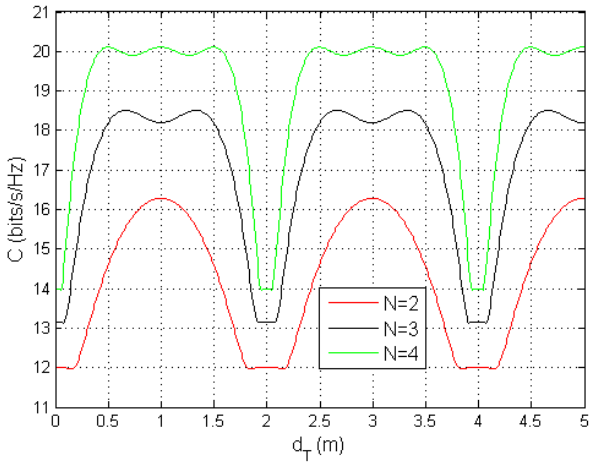

Fig. 5. Capacity with respect to d_T at 15 dB SNR with ideal DP antennas

The incremental capacity from increasing N can be traded-off to reduce each transmit antenna size and thus the uplink antenna gain term $g_{u,n}^{\text{ant}}$ in (11). For a parabolic antenna with diameter D and efficiency η the maximum antenna gain at boresight is given by:

$$g^{\text{ant}} = \frac{\sqrt{\eta}\pi D f}{c}. \tag{26}$$

Reducing each antenna size by $\sqrt{N}$, the combined overall antenna area $\sum^{N} \pi \left(\frac{D}{2\sqrt{N}}\right)^2$ remains the same irrespective of N. The effect on capacity of reducing the transmit antenna gain in equation (9) by scaling the antenna size is shown in Figure 6 with respect to d_T at 15 dB SNR. The benefit of using water-filling (WF) power allocation with respect to equal (EQ) power allocation is also compared in Figure 6.

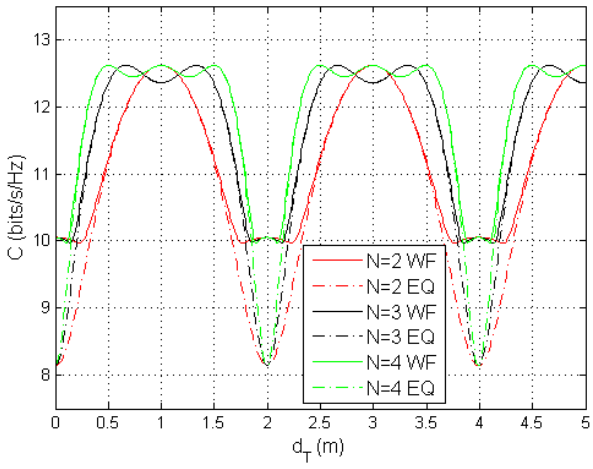

Fig. 6. Tx antenna size scaled with respect to N: Capacity with respect to d_T at 15 dB SNR with ideal DP antennas

In Figure 7, the water filling capacity for d_T values at 1m and 2m separations respectively are shown. At high SNR values ($>$ 9 dB), better capacity is achieved when $d_T = 1$m, which is an optimal d_T value for spatial multiplexing. However at low SNR values ($\leq$ 9dB), the capacity results are better at $d_T = 2$m, which is a non-optimal d_T value for spatial multiplexing but favourable to achieve power gain. Here the water-filling power allocation method benefits the capacity with power gain instead of spatial multiplexing. Single satellite SISO capacity is shown for comparison to appreciate the benefit of MIMO.

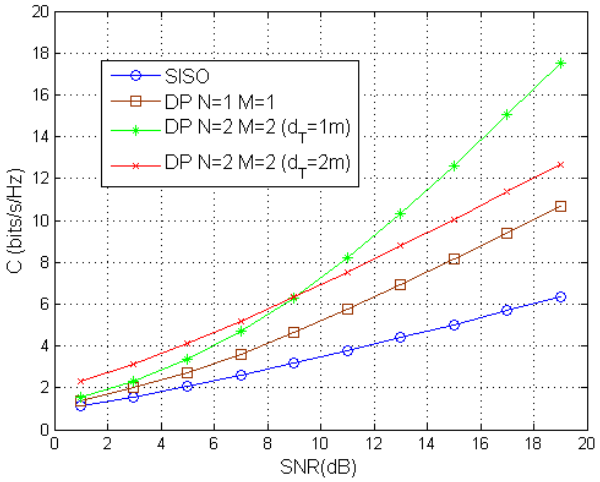

Fig. 7. Tx antenna size scaled with respect to N: Capacity with respect to SNR with ideal DP antennas

A. Polarization impact

Generally for circularly polarized SATCOM terminals, AR ≤ 1.5 dB is typical from antenna data sheets. In XPD terms this is equivalent to XPD ≤ -15 dB [6]. Discounting the polarization orientation error and if we assume each antenna has $\theta_2 = \theta_1$, the amplitude ($\frac{1}{1.3} \leq A \leq 1.3$) and phase ($-10^o \leq \psi \leq 10^o$) errors in these range have XPD ≤ -15 from equation (27) [9].

$$\text{XPD}_i = \frac{|\mathbf{p}_{l,ideal}^{\dagger}\mathbf{p}_i|^2}{|\mathbf{p}_{i,ideal}^{\dagger}\mathbf{p}_i|^2} = \frac{|A_i - e^{-j\psi_i}|^2}{|A_i + e^{-j\psi_i}|^2} \quad (l, i = 1, 2, \;\; l \neq i). \tag{27}$$

A random uniform error distribution in amplitude $U(\frac{1}{1.3}, 1.3)$ and phase $U(-10^o, +10^o)$ in equation (5) gives a histogram for p from -24 dB to -6 dB and mode lies at -9 dB. The effect of this value of p on the achievable capacity is shown in Figure 8. For $p = -9$ dB, approximately ten percent of the capacity is lost at high SNRs due to non-ideal DP antennas.

B. Ephemeris impact

So far we have assumed the satellites are fixed in their respective orbits, that is the satellites are always stationary with respect to the ground. However in practice the satellites do not maintain a stationary position due to non-zero eccentricity and inclination. A typical station keeping box for

Authorized licensed use limited to: Georgia Institute of Technology. Downloaded on January 12,2023 at 21:22:05 UTC from IEEE Xplore. Restrictions apply.

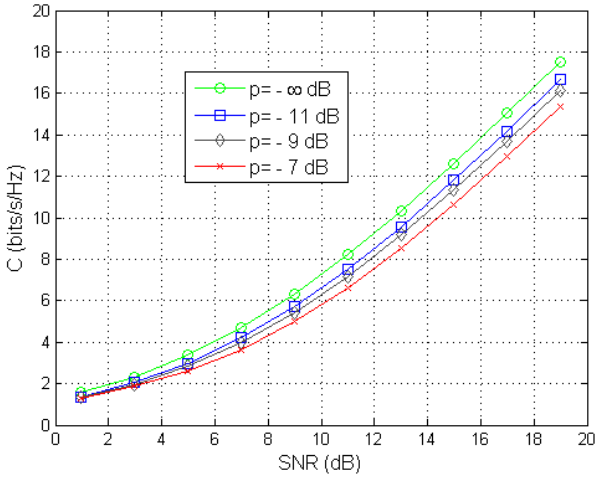

Fig. 8. Polarization impact on capacity at optimal d_T (1m) ($N = M = 2$)

a geostationary satellite in latitude and longitude is $\pm 0.05^{\text{o}}$ and $4e^{-4}$ in eccentricity [13]. An example orbit for each satellite within the station keeping box with an inclination $= 0.05^{\text{o}}$ degrees and eccentricity $= 4e^{-4}$ is shown in Figure 9 in normalized XYZ axes (physically the satellites occupy 156E and 157E orbital slots). The orbit for the second satellite is designed in reverse to the first satellite orbit (argument of perigee differs by 180^{o} degrees), to emulate the scenario that the two satellites are not always in the same plane with respect to the ground. The capacity analysis with respect to satellites in Figure 9 orbits and optimal $d_T = 1$ metre shows that the achievable capacity is always greater 99.98 percent of the optimum capacity. This gives confidence that the MIMO capacity has negligible degradation due to satellite movements within the station keeping box.

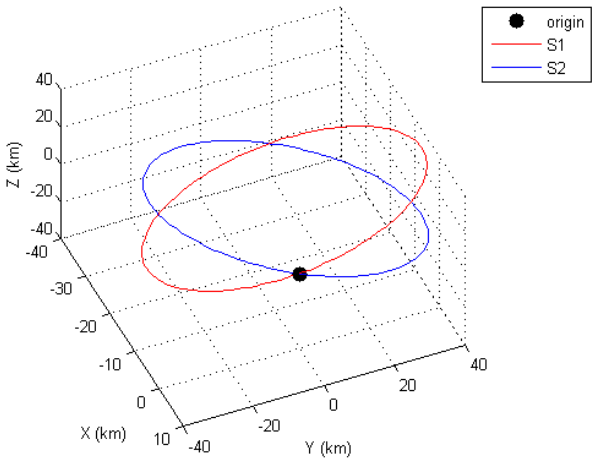

Fig. 9. Satellites in their respective orbits, in localized XYZ axes

V. Conclusions

In this paper we have presented a MIMO model for a line-of-sight (LOS) satellite communications (SATCOM) channel utilising orthogonal polarizations and spatial multiplexing. Although utilising orthogonal polarizations is a well known frequency reuse technique in SATCOM, the advantage of MIMO polarization is two-fold. The first is as a technique to counter poor cross polar isolation (XPI) and the second is to double the available spatial multiplexing gains. Generally, multiple satellites in the same frequency band do not operate in orbital slots less than two degrees apart due to adjacent satellite interference issues from small terminals. In this paper we show that by using MIMO the spatial channel capacity can be increased for satellites in close orbital slots. Capacity analysis shows that at high signal-to-noise ratio (SNR) significant capacity gain can be achieved through spatial multiplexing. However, at low SNR especially with channel state information available at the transmitter (CSIT) the MIMO channel benefits from power gain. The effect of satellite movements within station keeping boxes creates negligible impact on the achievable capacity.

References

[1] P. D. Arapoglou, K. Liolis, M. Bertinelli, A. Panagopoulos, P. Cottis, and R. De Gaudenzi, "MIMO over Satellite: A Review," *IEEE Journal on Communications Surveys and Tutorials*, vol. 13, no. 1, pp. 27–51, 2011.

[2] D. Tse and P. Vishwanath, *Fundamentals of Wireless Communications*. Cambridge University Press, 2005.

[3] R. T. Schwarz, A. Knopp, D. Ogermann, C. A. Hofinann, and B. Lankl, "Optimum-capacity MIMO satellite link for fixed and mobile services," in *International ITG Workshop on Smart Antennas, 2008. WSA 2008*, pp. 209–216.

[4] R. T. Schwarz, A. Knopp, D. Ogermann, C. A. Hofmann, and B. Lankl, "On the prospects of MIMO SatCom systems: The tradeoff between capacity and practical effort," in 6^{th} *International Multi-Conference on Systems, Signals and Devices, 2009. SSD '09.*, pp. 1–6.

[5] A. Knopp, R. T. Schwarz and B. Lankl, "MIMO system implementation with displaced ground antennas for broadband military SATCOM," in *Military Communications Conference, 2011 - MILCOM 2011*, pp. 2069–2075.

[6] L. Gonzalez, C. McLain, and W. Hall, "A plausible CONOPS for frequency reuse at Ka-band on WGS system," in *IEEE Military Communications Conference, MILCOM 2011*, pp. 1676–1683.

[7] B. Ramamurthy, W. G. Cowley, L. M. Davis, and G. Bolding, "Dual Polarization Frequency Reuse in SATCOM: A Method to Counter Poor Cross-Polar Isolation," in *IEEE Military Communications Conference, MILCOM 2014*, pp. 586–591.

[8] P. Wade, "Septum Polarizers and Feeds." W1GHZ, in Proc. of Microwave update, 2003, http://www.w1ghz.org/antbook/conf/SEPTUM.pdf.

[9] P.-S. Kildal., *Foundations of Antennas: A Unified Approach*. Studentlitteratur, Lund, 2000.

[10] M. Coldrey, "Modeling and Capacity of Polarized MIMO Channels," in *Vehicular Technology Conference, 2008. VTC Spring 2008. IEEE*, pp. 440–444.

[11] I. Gupta and A. Ksienski, "Effect of mutual coupling on the performance of adaptive arrays," *Antennas and Propagation, IEEE Transactions on*, vol. 31, no. 5, pp. 785–791, Sep 1983.

[12] E. Biglieri, R. Calderbank, A. Constantinides, A. Goldsmith, A. Paulraj, and H. V. Poor, *MIMO Wireless Communications*. Cambridge University Press, 2007.

[13] G. Maral. and M. Bousquet., *Satellite Communications Systems*. John Wiley, 4th ed., 2002.

Authorized licensed use limited to: Georgia Institute of Technology. Downloaded on January 12,2023 at 21:22:05 UTC from IEEE Xplore. Restrictions apply.